Effect of Strain and Diameter on Electronic and Charge Transport Properties of Indium Arsenide Nanowires

Pedram Razavi, James C. Greer

PII: S0038-1101(18)30091-1
DOI: https://doi.org/10.1016/j.sse.2018.08.001
Reference: SSE 7456

To appear in: *Solid-State Electronics*

Received Date: 31 January 2018
Revised Date: 27 July 2018
Accepted Date: 3 August 2018

Please cite this article as: Razavi, P., Greer, J.C., Effect of Strain and Diameter on Electronic and Charge Transport Properties of Indium Arsenide Nanowires, *Solid-State Electronics* (2018), doi: https://doi.org/10.1016/j.sse.2018.08.001

Effect of Strain and Diameter on Electronic and Charge Transport Properties of Indium Arsenide Nanowires

Pedram Razavi[1] and James C. Greer[1,2]
Tyndall National Institute, University College Cork, Lee Maltings, Dyke Parade, Cork, Ireland T12 R5CP
University of Nottingham Ningbo China, 199 Taikang East Road, Ningbo, 315100, China

Abstract — The impact of uni-axial compressive and tensile strain and diameter on the electronic band structure of indium arsenide (InAs) nanowires (NWs) is investigated using first principles calculations. Effective masses and band gaps are extracted from the electronic structure for zero strain and strained nanowires. Material properties are extracted and applied to determine charge transport described within the effective mass approximation and by applying the non-equilibrium Green's function method. The transport calculations self-consistently solve the Schrödinger equation with open boundary conditions and Poisson's equation for the electrostatics. The device structure corresponds to a metal oxide semiconductor field effect transistor (MOSFET) with an InAs NW channel in a gate-all-around geometry. The channel cross sections are for highly scaled devices within a range of 3×3 nm^2 to 1×1 nm^2. Strain effects on the band structures and electrical performance are evaluated for different NW orientations and diameters by quantifying subthreshold swing and ON/OFF current ratio. Our results reveal for InAs NW transistors with critical dimensions of a few nanometer, the crystallographic orientation and quantum confinement effects dominate device behavior, nonetheless strain effects must be included to provide accurate predictions of transistor performance.

1. Introduction

Field-effect transistors (FETs) are on target to be manufactured with sub-7 nm critical dimensions within the next few years[1]. Electronic properties of materials at these length scales vary significantly with respect to the bulk due to increase in the surface-to-volume ratio and quantization effects arising at small critical dimensions[2,3]. Due to large quantum confinement effects in NWs, there is substantial band gap widening relative to the bulk energy gap. In addition to band gap widening, the direct or indirect nature of a semiconducting material can be

altered due to band folding[4-6] leading to fundamentally different electrical and optical properties relative to the bulk. Improvement of the electrical performance and obtaining satisfactory electrical drive current in the highly-scaled MOSFETs requires technology boosters such as thin-body channels and strained nanowires, as well may require high transport channel materials such as germanium and/or III-V compound materials[7,8]. A feature of III-V semiconductors is the possibility to control the device dimensions, doping concentrations, and material composition while achieving band gap engineering during fabrication[9,10]. However when scaling any MOSFET architecture, a set of deleterious performance issues such as degradation of subthreshold swing (SS) and ON/OFF current ratio (I_{ON}/I_{OFF}) emerge which are collectively referred to as short-channel effects (SCEs)[11]. Nanowire structures with a gate electrode wrapped around the NW axis, known as the gate-all-around (GAA) configuration, enhances electrostatic control of the channel carriers and considerably mitigates against short-channel effects for highly scaled dimensions[7]. III-V materials maintain very high electron mobility together with good drive currents in NW field-effect-transistors (FETs)[12] and substantial progress on the fabrication of III-V NW devices on a Si substrate has been achieved in recent years[13]. However in devices scaled below 7 nm critical dimensions, extrapolations based on bulk and classical device concepts need to be tested[1]. The impact of strain in NWs can considerably affect device characteristics beyond what is observed at larger dimensions for physical properties such as the band gap and effective masses, and these effects are strongly dependent on the crystallographic orientation of the nanowire primary axis[14]. Moreover, strain engineering is well known to be capable of improving charge carrier mobility in semiconducting materials[14]. However, unlike the group IV semiconductors silicon and germanium as well as their alloys, there is less known about the effect of strain on the physical properties of III-V nanowires[4,6,15-18], particularly in the context of nanoelectronic devices. To this end, the band structures of InAs nanowires are investigated with the goal of extracting accurate transport models for nanowire transistors[19] with cross sections in the range of approximately 3×3 nm^2 to 1×1 nm^2. Different wire orientations are considered and the effect of strain is also evaluated through the use of density functional theory (DFT) calculations. Quantum transport simulations are also performed to obtain the transfer characteristics of transistors with InAs nanowire channels and subthreshold swings (SS), and drive currents (I_{ON}) are extracted.

2. Methods

The DFT calculations are performed using a linear combination of atomic orbitals (LCAO) consisting of a polarized double-zeta basis set. A meta-generalized gradient approximation (meta-GGA) for the exchange-correlation functional in the DFT calculations is used[20-22]. The energy band gap of bulk InAs is relatively narrow at room temperature (E_g=0.354 eV)[19] and the well-known band gap underestimation of standard approximations to the exchange-correlation functionals such as the local density approximation or generalized gradient approximation (GGA) make their use unsuitable for narrow gap semiconductors. The importance of an accurate treatment of the kinetic energy density for the calculation of band gaps in solids using density functional theory is also known[23]. Meta-GGA[24] functionals relate the exchange-correlation energy at each point not only to the local electronic density, but also to the electronic density gradient and the Kohn-Sham kinetic energy density. As a result, meta-GGA functionals can provide a more accurate band gap prediction, however at the expense of an empirical calibration. By fitting the "c"-parameter of the Tran and Blaha exchange–correlation functional[24], the energy band gap for bulk InAs is calibrated to the experimental value of 0.354 eV [19]. By doing so we obtain the effective mass of 0.023 in good agreement with effective mass of 0.026 from ref.19. For all nanowire calculations, a Monkhorst-Pack sampling[25] with a 23×1×1 *k*-point grid and energy cut-off of 100 Hartree is used to generate the real-space grid and for bulk calculations 13×13×13 *k*-point grid were used. The total electronic energy for each NW is minimized with respect to atomic positions. The atomic configurations are relaxed to a force of less than 0.01 $eVÅ^{-1}atom^{-1}$ and the resulting geometries are taken as the zero strain reference configurations.

Electron effective masses at conduction band minima are calculated using a parabolic approximation with a second derivative $\partial^2 E/\partial k^2$ determined using a 5 point stencil method[26]. Approximately square zinc-blend (ZB) InAs nanowires are generated with wire orientations of [100], [110] and [111] with cross-sectional areas of approximately 3×3 nm^2 to 1×1 nm^2. The NW surfaces are passivated using pseudo-hydrogen atoms[27] to ensure passivation of all surface dangling bonds thus avoiding issues relating to specific surface chemistry and bonding on the electronic properties of the NWs – in this sense the calculations provide a reference for the ideal surface termination. Figure 1 shows typical cross sectional views of the relaxed InAs NWs for different wire orientations used in our study.

3. Electronic structure results

To determine the effect of the wire cross section and orientation on characteristics of InAs nanowires at low critical dimensions, the band gaps and effective masses are extracted from the meta-GGA electronic structures and plotted in figure 2a; these are the two critical parameters for determining transistor performance as the band gap widening due to quantum confinement governs thermal and tunneling properties thus influencing ON/OFF current ratios, and electron effective masses can be considered as a first approximation to the changes in electron mobility, with smaller effective masses correlating to higher electron mobility. To examine the effect of the band gap correction using the meta-GGA functional affect these parameters, values extracted from the LDA band structures are also plotted in figure 2a for comparison.

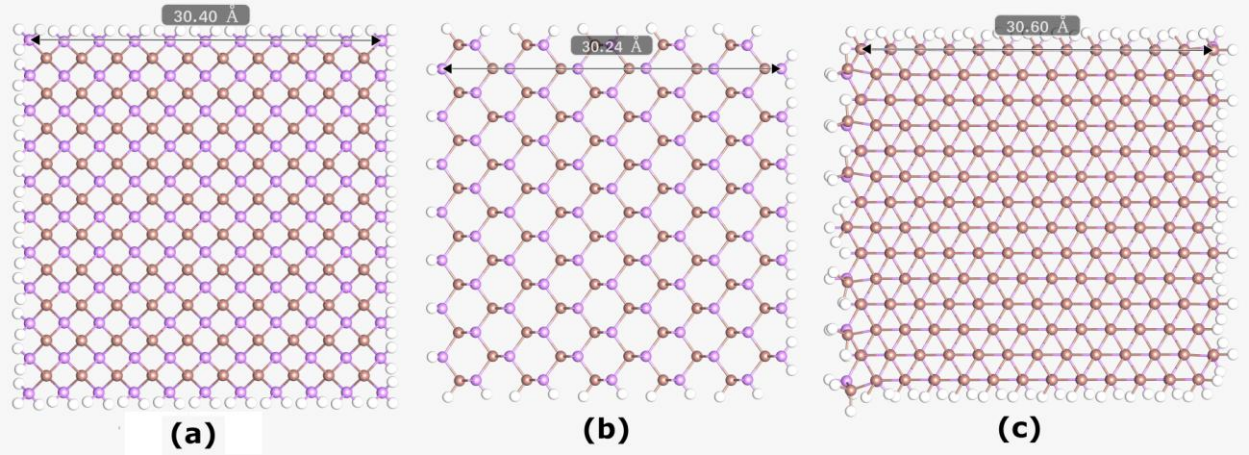

FIG. 1. Cross-section of InAs NWs for (a) [100], (b) [110], and (c) [111] wire orientations composed of As (pink), In (brown) and pseudo-H (white) atoms. Note that pseudo-hydrogens of appropriate charge are chosen for each surface atom to provide a defect free surface.

It can be seen that unlike bulk InAs which has isotropic effective mass at the Γ-point, for small diameter InAs nanowires the effective masses at Γ are not isotropic and wires with different orientations have different effective masses due to the large quantum confinement effects normal to the NW principal axis. Fig. 2b shows the band structures of 1 nm and 3 nm nanowires with different wire orientation in which the effect of quantum confinement on the band gap and the effective masses can be seen. The band gap and effective masses are highly dependent on

nanowire diameter and orientation which are the first indication of the impact these physical parameters for the electrical and optical properties of nanoscale NWs.

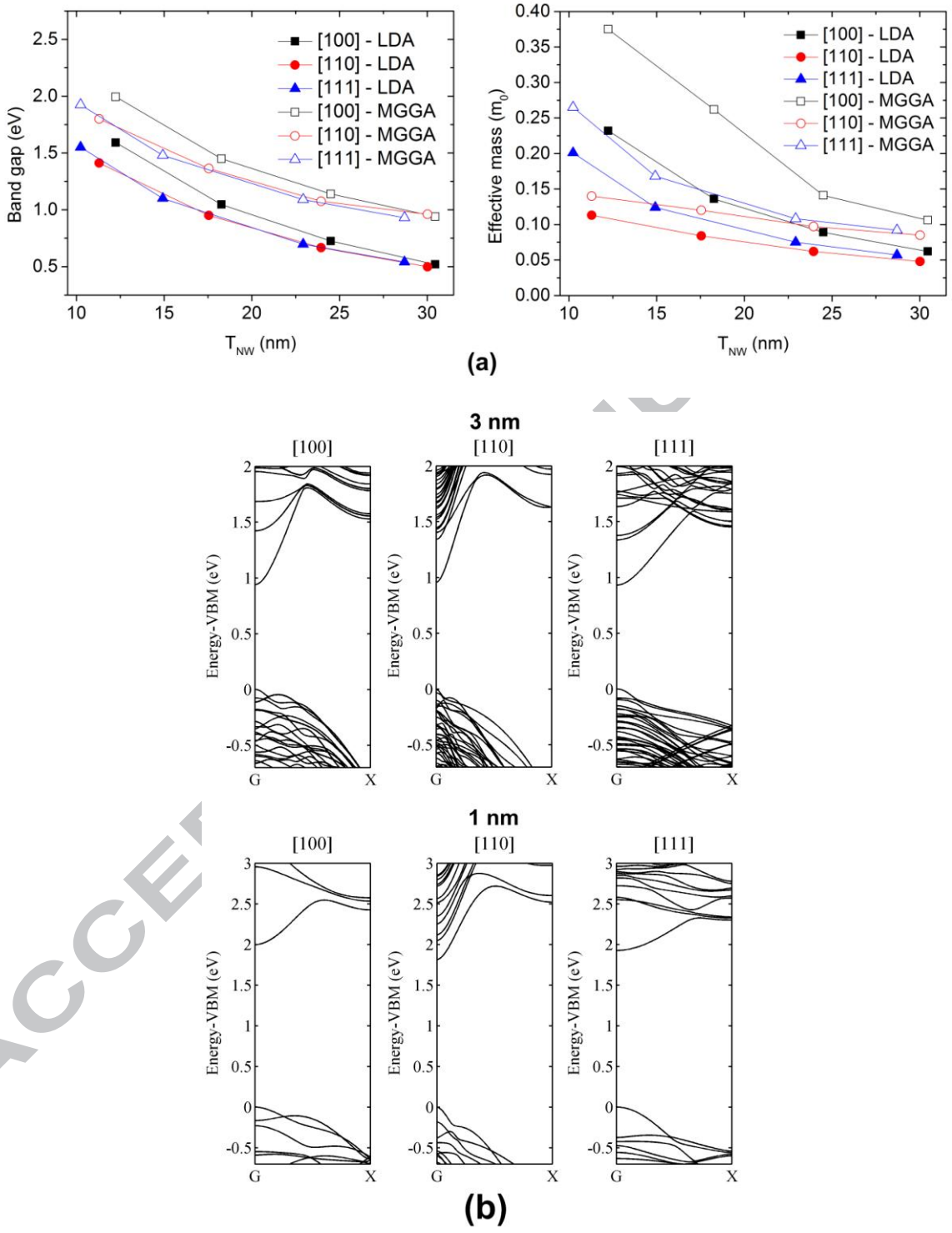

FIG. 2. Comparison of (a) band gaps and effective masses and (b) band structure of approximate 1×1 nm^2 and 3×3 nm^2 InAs NWs with different cross-section diameters and wire orientations. Note that the Meta-GGA approximation

as anticipated predicts a larger band gap than the LDA calculations, as well, the effective masses tend to be slightly larger within the Meta-GGA calculations. T_{NW} dentoes the length of a side of the approximately square InAs NWs.

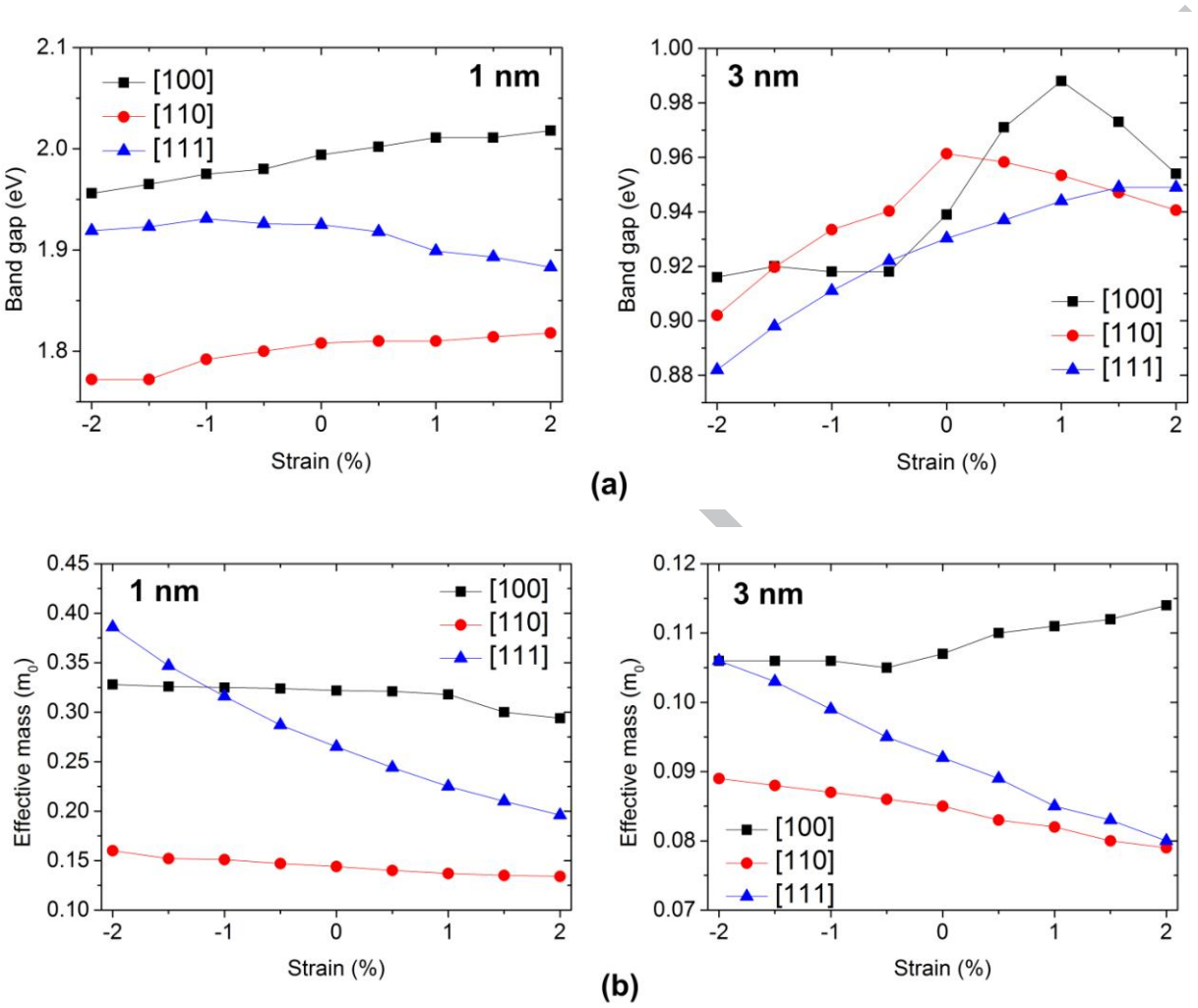

FIG. 3. Comparison of (a) band gaps and (b) effective masses for InAs NWs under compressive and tensile strains (up to ±2%).

Next, the effect of strain on the band structure of InAs nanowires is investigated as tensile and compressive uni-axial strains of up to ±2% are applied along the NW principal axe. Fig. 3 illustrates the results of applying strain to the NWs in terms of the effect on the band gap energies and effective masses; clearly the larger impact on the NW properties is due to NW orientation and the cross sectional area. However it should be noted the effect of tensile and compressive strains on the effective masses of the [111]-orientated NWs is found to be particularly large relative to the other NW orientations as illustrated in Fig. 4.

TABLE 1. Effect of tensile and compressive uniaxial strain on band gap and effective mass of InAs nanowires.

	(nm)	Compressive strain	E_g	m_e	Tensile strain	E_g	m_e
[100]	1	-2%	-1.9%	1.9%	2%	1.2%	-8.7%
	3	-1%	-2.3%	-1%	1%	5.2%	3.7%
		-2%	-2.6%	-1%	2%	1.6%	6.5%
[110]	1	-2%	-2%	8.3%	2%	0.6%	-7%
	3	-2%	-6.2%	4.7%	2%	2.2%	-7.1%
[111]	1	-2%	- 0.3%	45.7%	2%	-2.2%	-26%
	3	-2%	-5.2%	15.2%	2%	2%	-13%

As it shown in Fig. 3, the band gap of 3 nm [100]-oriented wire behaves differently from other orientations as a resulting of band folding in the directions normal to the NWs' principal axe. Applying tensile strain up to 1% increases the band gap and applying strain of 2% decreases the band gap. This results from band crossing as shown in Fig. 4c. Table 1 summarizes the change on band gap and effective mass of InAs nanowires (in percent) as a result of tensile and compressive uniaxial strain.

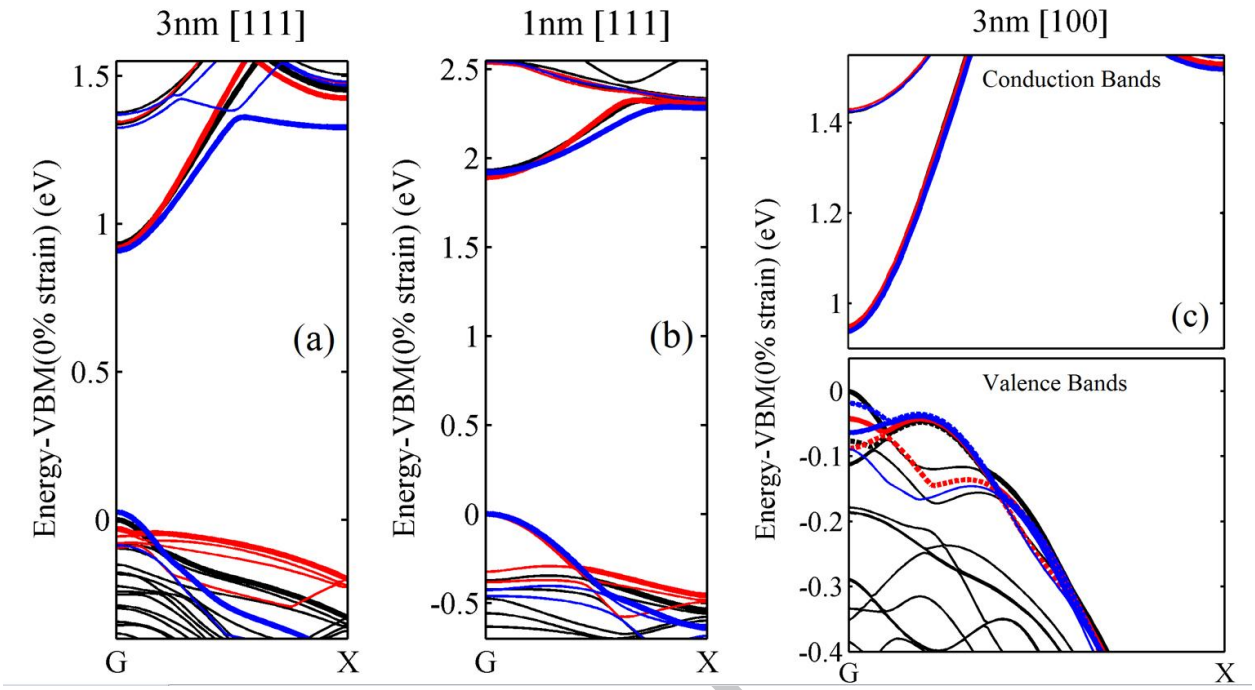

Fig. 4 (a) and (b) Band structures of [111]-oriented wires under 2% tensile (red) and 2% compressive (blue) strains. And (c) band crossing in valence bands of 3nm [100]-oriented wire by applying 1% (red) and 2% (blue) tensile strains. Note: black band structures are the band structures for the relaxed geometry.

These results reveal how wire orientation, diameter, and strain as applied (wanted) or due to the fabrication process (unwanted) affect electrical properties of transistor made with these narrow cross section InAs nanowires.

4. Charge transport results

The I-V characteristics of InAs gate-all-around nanowire transistors under tensile and compressive uni-axial strain (±2%) are calculated based on a self-consistent solution of the Schrodinger and Poisson equations via the non-equilibrium Green's function approach and effective mass approximation. Details about the method and implementation of the quantum transport calculations are given elsewhere[7]. The NW effective masses and band energies of the first 8 conduction subbands are extracted from the DFT-determined electronic structure calculations using the Meta-GGA approximation. The electronic structure results define the effective mass Hamiltonian. The subthreshold swing (SS) measures the rate of current increase with gate voltage below threshold, which is of particular importance to assess low power performance in ultra-scaled devices[28]. The SS along with the I_{ON}/I_{OFF} ratio are calculated as the

relative performance indicators for the different InAs transistors that are evaluated in the charge transport calculations. The supply voltage is fixed at V_{dd}=0.65 V and the gate work function is chosen for each nanowire transistor such that the off-current is 10 pA/μm at V_{gs}= 0 V which is suitable target for low standby power technologies[7]. The gate length and source/drain regions are 10 and 15 nm, respectively, the gate oxide thicknesses are 1 nm and the dielectric constants is chosen as 3.9. Uniform doping concentrations in the source/drain regions of 10^{20} cm^{-3} for approximately 3×3 nm^2 wires and $6x10^{20}$ cm^{-3} for the approximate 1.2×1.2 nm^2 cross sections are chosen to obtain a similar number of dopant atoms in source/drain regions for both structures. This results in scaling of the dopant concentration with nanowire cross section.

Fig. 5 shows the transfer characteristics of the InAs NWs. Table 2 summarize the values of the subthreshold swing and I_{on}/I_{off} ratios for the gate-all-around (GAA) configuration InAs nanowire transistors for different NW orientations and cross sections. From table 2 it is found that at a fixed gate length of 10 nm, as the cross-section decreases the subthreshold swing approaches the theoretical limit for room temperature operation of 59.6 mV/decade. This is a direct consequence of the better electrostatic control of the gate over charge carriers in devices with smaller cross-sections as can be explained by the natural length for multi-gate architectures[11]. It is also found that for the larger cross-section devices, the [100]-oriented InAs NW channel results in a lower SS of the three orientations considered, with the [111]-oriented NW channels intermediate, and [110]-oriented channels show the largest SS. These results can be explained by the findings for the effective masses in the transport direction (Fig. 2a) with a larger effective mass in the transport direction reducing source-to-drain tunneling and thereby improving the SS.

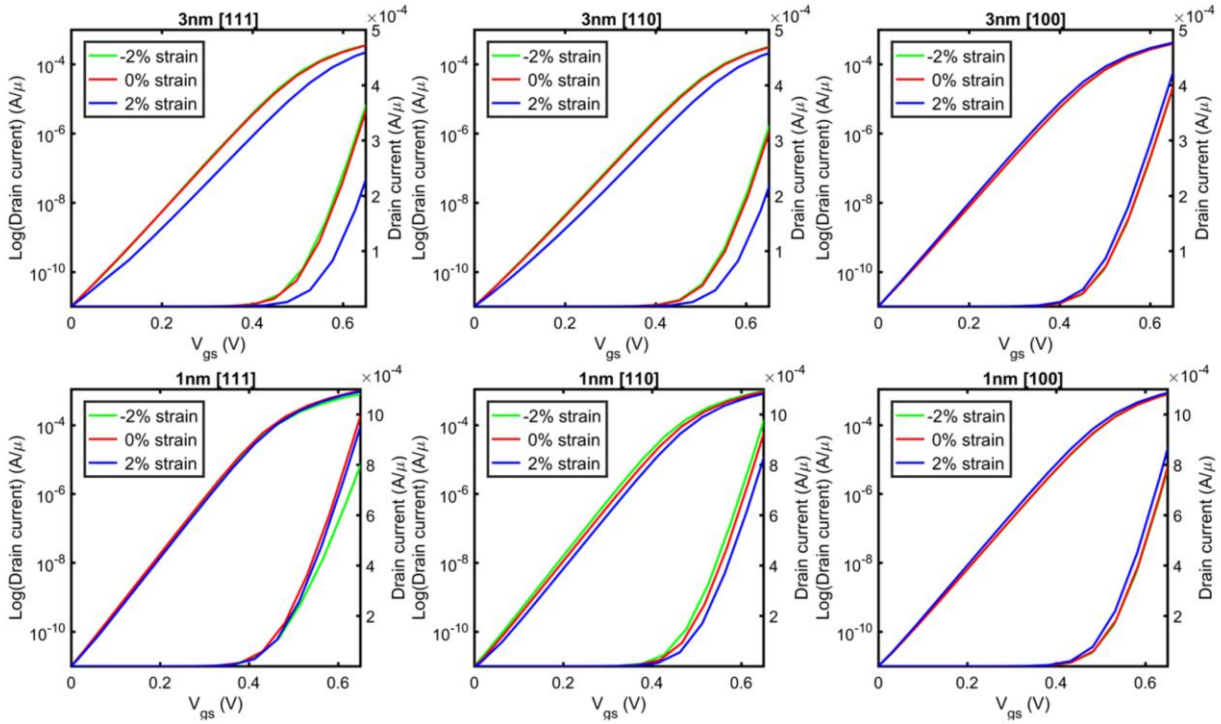

FIG. 5. Transfer characteristics of InAs NWs (L_{gate}=10 nm L_{sd}=15 nm).

Table 2 reveals that strain has a significant effect on the electrical properties of the InAs nanowire transistors at ultra-scaled dimensions, and the effect of strain is strongly coupled to NW orientation and critical dimensions. It is found that small cross section [111]-oriented InAs NWs are most sensitive to the effect of strain, particularly in reference to the influence of strain on effective mass.

TABLE 2. Subthreshold swing, and I_{on}/I_{off} of GAA InAs nanowire transistors (Ion extracted at V_{gs}=0.65 V and I_{off} is fixed at 10 pA/um).

		SS (mV/decade)			I_{on}/I_{off}		
		-2%	0%	2%	-2%	0%	2%
[100]	1nm	60.9	60.9	61	7.82×10^{7}	7.88×10^{7}	8.61×10^{7}
	3nm	68.2	67.9	66.7	3.94×10^{7}	3.96×10^{7}	4.22×10^{7}
[110]	1nm	61.9	62.9	63.5	9.97×10^{7}	9.91×10^{7}	8.49×10^{7}
	3nm	71.6	72.1	76.1	3.24×10^{7}	3.13×10^{7}	2.16×10^{7}
[111]	1nm	60.4	61.2	61.6	7.95×10^{7}	9.93×10^{7}	9.49×10^{7}
	3nm	68.7	70.2	74.8	3.61×10^{7}	3.52×10^{7}	2.28×10^{7}

5. Conclusions

We have investigated the effect of wire orientation and cross-section on the electrical properties of ultrascaled InAs nanowires under uniaxial tensile and compressive strain. These results illustrate how wire orientation, diameter, and how applied strain (wanted) or due to the fabrication processes (unwanted) can affect electrical properties of the transistors made with narrow cross section InAs nanowires. Unlike bulk InAs which has isotropic effective mass at the Γ-point, the effective masses at Γ for small diameter InAs nanowires are not isotropic due to the large quantum confinement effects. However with increasing wire diameters effective mass values of different orientations become more isotropic and return to the bulk value. MetaGGA functionals are used for an accurate treatment of band gap energies. It is shown that the band gap and effective masses are highly dependent on nanowire diameter and orientation and this dependence has been quantified. Our results illustrate applying tensile and compressive uniaxial strain to the [111]-oriented NWs is found to particularly affect effective masses for nanowire cross sections of approximately 1×1 nm^2, and as a result have a significant impact on the current-voltage transfer characteristics. The results show that strain engineering can be used to improve device characteristics just as is commonly performed for silicon technologies. On the other hand, the large effect of strain on physical properties of these InAs NWs also suggests that controlling process induced strain will be critical to maintaining uniform device characteristics.

ACKNOWLEDGMENTS

This work was supported by the European Union project DEEPEN funded under NMR-2013-1.4-1 grant agreement number 604416. We also wish to acknowledge the SFI/HEA Irish Centre for High-End Computing (ICHEC) for the provision of computational facilities and a Science Foundation Ireland Investigator Award 13/IA/1956.

REFERENCES

1 Razavi, P. *et al.* Influence of channel material properties on performance of nanowire transistors. *Journal of Applied Physics* **111**, 124509-124509-124508 (2012).

2 Ansari, L., Feldman, B., Fagas, G., Colinge, J.-P. & Greer, J. C. Simulation of junctionless Si nanowire transistors with 3 nm gate length. *Applied Physics Letters* **97**, 062105-062103 (2010).

3 Ferain, I., Colinge, C. A. & Colinge, J.-P. Multigate transistors as the future of classical metal-oxide-semiconductor field-effect transistors. *Nature* **479**, 310-316 (2011).

4 Copple, A., Ralston, N. & Peng, X. Engineering direct-indirect band gap transition in wurtzite GaAs nanowires through size and uniaxial strain. *Applied Physics Letters* **100**, 193108, (2012).

5 Signorello, G. *et al.* Inducing a direct-to-pseudodirect bandgap transition in wurtzite GaAs nanowires with uniaxial stress. *Nature Communications* **5**, 3655, (2014).

6 Peng, X. & Copple, A. Origination of the direct-indirect band gap transition in strained wurtzite and zinc-blende GaAs nanowires: A first principles study. *Physical Review B* **87**, 115308 (2013).

7 Razavi, P. *et al.* Influence of channel material properties on performance of nanowire transistors. *Journal of Applied Physics* **111**, 124509, (2012).

8 Razavi, P. & Fagas, G. Electrical performance of III-V gate-all-around nanowire transistors. *Applied Physics Letters* **103**, 063506, (2013).

9 Khayer, M. A. & Roger, K. L. *Journal of Applied Physics* 107, 014502, (2010).

10 Tomioka, K., Yoshimura, M. & Fukui, T. A III-V nanowire channel on silicon for high-performance vertical transistors. *Nature* **488**, 189-192, (2012).

11 Colinge, J. P. & Greer, J. C. *Nanowire Transistors: Physics of Devices and Materials in One Dimension*. (Cambridge University Press, 2016).

12 Jiang, X. *et al.* InAs/InP Radial Nanowire Heterostructures as High Electron Mobility Devices. *Nano Letters* **7**, 3214-3218, (2007).

13 Tomioka, K., Tanaka, T., Hara, S., Hiruma, K. & Fukui, T. III–V Nanowires on Si Substrate: Selective-Area Growth and Device Applications. *IEEE Journal of Selected Topics in Quantum Electronics* **17**, 1112-1129, doi:10.1109/JSTQE.2010.2068280 (2011).

14 Niquet, Y.-M., Delerue, C. & Krzeminski, C. Effects of Strain on the Carrier Mobility in Silicon Nanowires. *Nano Letters* **12**, 3545-3550, (2012).

15 Zardo, I. *et al.* Pressure Tuning of the Optical Properties of GaAs Nanowires. *ACS Nano* **6**, 3284-3291, (2012).

16 Conzatti, F., Pala, M. G., Esseni, D., Bano, E. & Selmi, L. Strain-Induced Performance Improvements in InAs Nanowire Tunnel FETs. *IEEE Transactions on Electron Devices* **59**, 2085-2092, (2012).

17 Cheung, H.-Y. *et al.* Modulating Electrical Properties of InAs Nanowires via Molecular Monolayers. *ACS Nano* **9**, 7545-7552, (2015).

18 Razavi, P. & Greer, J. C. Influence of surface stoichiometry and quantum confinement on the electronic structure of small diameter InxGa1-xAs nanowires. *Materials Chemistry and Physics* **206**, 35-39, (2018).

19 Zerveas, G. *et al.* Comprehensive comparison and experimental validation of band-structure calculation methods in III–V semiconductor quantum wells. *Solid-State Electronics* **115, Part B**, 92-102, (2016).

20 Atomistix ToolKit version 2016 QuantumWise A/S, w. q. c.

21 Brandbyge, M., Mozos, J.-L., Ordejón, P., Taylor, J. & Stokbro, K. Density-functional method for nonequilibrium electron transport. *Physical Review B* **65**, 165401 (2002).

22 José, M. S. *et al.* The SIESTA method for ab initio order- N materials simulation. *Journal of Physics: Condensed Matter* **14**, 2745 (2002).

23 Tran, F. & Blaha, P. Importance of the Kinetic Energy Density for Band Gap Calculations in Solids with Density Functional Theory. *The Journal of Physical Chemistry A* **121**, 3318-3325, doi:10.1021/acs.jpca.7b02882 (2017).

24 Tao, J., Perdew, J. P., Staroverov, V. N. & Scuseria, G. E. Climbing the Density Functional Ladder: Nonempirical Meta Generalized Gradient Approximation Designed for Molecules and Solids. *Physical Review Letters* **91**, 146401 (2003).

25 Monkhorst, H. J. & Pack, J. D. Special points for Brillouin-zone integrations. *Physical Review B* **13**, 5188-5192 (1976).

26 Abramowitz, M. *Handbook of Mathematical Functions, With Formulas, Graphs, and Mathematical Tables*. (Dover Publications, Incorporated, 1974).

27 Huang, X., Lindgren, E. & Chelikowsky, J. R. Surface passivation method for semiconductor nanostructures. *Physical Review B* **71**, 165328 (2005).

28 Skotnicki, T. & Boeuf, F. in *VLSI Technology (VLSIT), 2010 Symposium on.* 153-154.

Pedram Razavi received the Ph.D. degree in electrical and electronic engineering from Tyndall National Institute, University College Cork, Ireland in 2013. He is currently a Postdoctoral Researcher with the Tyndall National Institute, University College Cork, Ireland, working on the design and analysis of high-speed high-sensitivity photodetectors. He previously worked on the multiscale simulation capability for predictive design of novel materials and nanostructures modeling.

Highlights

- The band gap and effective masses are highly dependent on NW diameter and orientation
- Strain particularly affect effective masses of the 1×1 nm^2 [111]-oriented NWs
- Strain engineering can improve device characteristics in InAs nanowires
- Controlling process induced strain is critical for uniform device characteristics.